

γ -ray fluxes in Oklo natural reactors

C. R. Gould*

*Physics Department, North Carolina State University, Raleigh, North Carolina 27695-8202, USA and
Triangle Universities Nuclear Laboratory, Durham, North Carolina 27708-0308, USA*

E. I. Sharapov

Joint Institute for Nuclear Research, 141980 Dubna, Moscow Region, Russia

A. A. Sonzogni

National Nuclear Data Center, Brookhaven National Laboratory, Upton, New York 11973-5000, USA

(Received 5 July 2012; revised manuscript received 4 October 2012; published 5 November 2012)

Background: Uncertainty in the operating temperatures of Oklo reactor zones impacts the precision of bounds derived for time variation of the fine structure constant α . Improved $^{176}\text{Lu}/^{175}\text{Lu}$ thermometry has been discussed but its usefulness may be complicated by photoexcitation of the isomeric state ^{176m}Lu by $^{176}\text{Lu}(\gamma, \gamma')$ fluorescence.**Purpose:** We calculate prompt, delayed, and equilibrium γ -ray fluxes due to fission of ^{235}U in pulsed mode operation of Oklo zone RZ10.**Methods:** We use Monte Carlo modeling to calculate the prompt flux. We use improved data libraries to estimate delayed and equilibrium spectra and fluxes.**Results:** We find γ -ray fluxes as a function of energy and derive values for the coefficients $\lambda_{\gamma, \gamma'}$ that describe burn-up of ^{176}Lu through the isomeric ^{176m}Lu state.**Conclusion:** The contribution of the (γ, γ') channel to the $^{176}\text{Lu}/^{175}\text{Lu}$ isotopic ratio is negligible in comparison to the neutron burn-up channels. Lutetium thermometry is fully applicable to analyses of Oklo reactor data.DOI: [10.1103/PhysRevC.86.054602](https://doi.org/10.1103/PhysRevC.86.054602)

PACS number(s): 06.20.Jr, 07.05.Tp, 25.20.Dc, 25.85.Ec

I. INTRODUCTION

Studies of the ^{235}U fission product isotopic ratios from Oklo [1] have been undertaken by many groups investigating whether the fine structure constant α has changed over the two billion years period since the reactors operated. As first pointed out by Shlyachter [2], the samarium isotopic ratios are sensitive to the value of α through the overlap of the ^{149}Sm $E_0 = 97.3$ meV neutron resonance with the thermal and epithermal portions of the neutron flux in the reactor. While the majority of Oklo analyses [3–7] have been consistent with no shift in the resonance energy, and therefore no change in α , a change has been argued for from astronomical observations [8].

All Oklo analyses make assumptions about the operating temperatures of the reactors, but there is as yet no agreement on what these temperatures actually were. Utilizing the $^{176}\text{Lu}/^{175}\text{Lu}$ isotope ratio method to determine temperatures was recently revisited by Gould and Sharapov [9]. The method is based on the temperature dependence of the large thermal neutron capture cross section of ^{176}Lu (natural abundance 2.599% [10]) and on knowing with certainty the (small) ground-state branching ratio for thermal neutron capture on the more abundant lutetium isotope, ^{175}Lu (natural abundance 97.401%). The dominant capture branch σ_{175}^m leads to a short-lived isomeric state in ^{176m}Lu , while only a minor branch σ_{175}^g leads to the ground state of ^{176}Lu . The data from Oklo show clearly that ^{176}Lu is depleted in the reactor zones, but as concluded in Ref. [9], the degree of depletion will be

a reliable indicator of the temperature only if an improved measurement of $B^g(175) = \sigma^g/(\sigma^g + \sigma^m)$ is performed and if alternate explanations [9] for depletion are ruled out.

One alternate explanation for ^{176}Lu depletion lies in the possibility of processing the lutetium isotopes in Oklo due to photoexcitation of the isomeric state in ^{176m}Lu by $^{176}\text{Lu}(\gamma, \gamma')$ fluorescence. Such a process is well known in astrophysics and is an important channel for burning ^{176}Lu in stellar environments [11,12]. The isomeric state decays to ^{176}Hf with a half-life of 3.6 h and therefore provides an alternate path for removing ^{176}Lu . Here we explore whether this could have been an effect in the γ -ray fluxes in the reactors, taking advantage of newly developed data libraries for fission decay chains.

In ^{235}U thermal neutron fission, about 6.6 MeV is released in the form of prompt γ rays, about 6.5 MeV as β rays, and about 6.3 MeV as γ rays following β emission. The sum of the delayed β and γ energy released during the decay of fission products is called decay heat and varies as a function of time, $f(t)$, after a single fission event at $t = 0$.

Beginning with the work of Way and Wigner [13], many calculations and measurements of $f(t)$ have been performed; see Tobias [14] and Dickens [15] for reviews. Typically, $f(t) \sim t^{-1.2}$ is found for times greater than several seconds.¹ With the development of more comprehensive nuclear data libraries based on level schemes derived from high-resolution Ge-detector data, summation method calculations have become widely accepted. These calculations give good agreement with measurements except at the shorter times associated with high

*chris_gould@ncsu.edu

¹Note this is not the same as the time dependence of decay heat following shutdown of a long-running reactor [16].

Q -value β decays. High Q values feed levels at high excitation that can decay by emission of weak and/or high-energy γ rays easily missed in Ge-detector measurements. As a result, the libraries were incomplete. Recently, total absorption γ spectrometer (TAGS) data have been included in libraries. This has eliminated the discrepancies. In particular, Algorta *et al.* [17] were able to report ^{239}Pu decay heat calculations in excellent agreement with experiments for shorter times.

We follow this approach for calculating ^{235}U decay heat γ spectra [18], converting to fluxes using standard energy deposition conversion coefficients. We apply Monte Carlo modeling to calculate the prompt γ -ray flux in the Oklo reactor zone. With these fluxes in hand and a model of how the reactor operated, we can then estimate photoexcitation constants $\lambda_{\gamma,\gamma'}$ for burning ^{176}Lu through the isomeric state ^{176m}Lu .

II. PROMPT FISSION γ -RAY FLUX IN OKLO REACTOR ZONE RZ10

The MCNP code [19] allows modeling of neutron transport and also provides the energy dependence of the prompt γ -ray flux. We use the same input for the Oklo zone RZ10 as in our previous work [5]. The model of a reactor zone is a flat cylinder 70 cm high and 6 m in diameter, surrounded by a 1-m-thick reflector consisting of water-saturated sandstone. As for any reactor, Oklo criticality is determined by the geometry and the composition of the active zone. Oklo reactor zones include uraninite UO_2 , gangue (oxides of different metals with water of crystallization), and water. The total density of the active

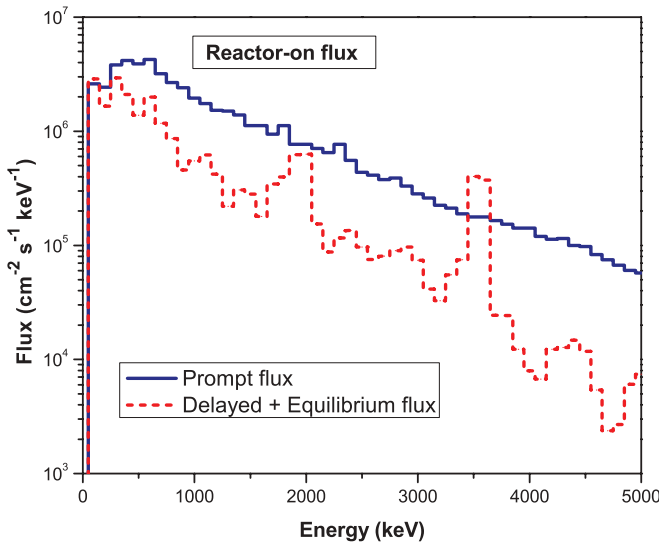


FIG. 1. (Color online) Prompt and delayed γ -ray fluxes $\Phi_\gamma(E)$ in Oklo reactor zone RZ10 during the period the reactor is on. The fluxes are calculated for an 18-kW reactor cycling on for 0.5 h and off for 2.5 h. The prompt flux, from MCNP, is the upper line. The lower line is the delayed flux for one 0.5-h fresh-core reactor-on pulse, multiplied by 1.31 to take into account the equilibrium flux associated with the N previous reactor-on pulses ($N \gg 1$). The statistical uncertainty in the prompt spectrum simulation is 5%. The structure in the delayed flux is due to incomplete averaging of contributions from the discrete lines shown in Fig. 3.

core material at ancient times was about 3 g cm^{-3} for RZ10 with only 30 wt% of UO_2 in the RZ10 dry ore. The hydrogen to uranium atomic ratio in our model was $\frac{N_H}{N_U} = 13.0$ and the multiplication coefficient of the fresh core was $k_{\text{eff}} = 1.036$. Detailed composition and neutronic parameters of the RZ10 reactor zone are given in Ref. [5]. The rate of fission can be deduced from the Hidaka and Holliger model [20], which found an average RZ10 neutron fluence of 0.65 kb^{-1} over a time duration of 160 kyr.

From analysis of xenon isotope abundances in Oklo grains of aluminum phosphate, Meshik *et al.* [21] concluded the reactors operated cyclically, with reactor-on periods of about 0.5 h (1800 s), separated by dormant reactor-off periods of 2.5 h (9000 s). We use this periodicity in calculating absolute fluxes. Adapting to the pulse mode, we find 1.03×10^{18} fissions for the 1800 s the reactor is on, with a thermal power of about 18 kW. We include only ^{235}U fission here since ^{238}U and ^{239}Pu fission was found by Hidaka and Holliger to contribute less than 10% to the neutron yields.

The prompt γ -ray flux during the reactor-on period is shown as the upper line in Fig. 1. The other flux shown refers to the delayed heat and is discussed in the next sections. The total prompt γ -ray flux is about $3 \times 10^9 \text{ } \gamma \text{ cm}^{-2} \text{ s}^{-1}$. The electromagnetic energy per fission corresponds to about 14.7 MeV, greater than the 6.6 MeV of prompt γ -ray fission energy due to neutron capture on the materials of the reactor.

III. DECAY HEAT γ -RAY SPECTRA FROM FISSION

A large number of radioactive nuclides are produced from the fission of an actinide target such as ^{235}U . Of relevance in describing the time evolution of the decay network are the longer lived levels, ground states, and isomers, here called *materials*. While the reactor is operating, the *materials* population satisfies the following set of linearly coupled differential equations:

$$\frac{dN_i(t)}{dt} = -\lambda_i N_i(t) + \sum_k \lambda_k P_{ki} N_k(t) + r Y_i, \quad (1)$$

where the decay constant of the material i is $\lambda_i = \ln(2)/t_{1/2i}$, $t_{1/2i}$ is the half-life for the material i , P_{ki} is the probability that the material k will populate in its decay the material i , r is the fission rate, and Y_i is the independent fission yield for the material i . When the reactor is not operating, the equations for $N_i(T)$ are the same but with $r = 0$.

For each material, we have obtained the Ge-detector γ -ray spectrum $I_i(E_\gamma)$ from the ENDF/B-VII.1 decay data sublibrary [22], using a detector resolution of 2 keV (FWHM) for discrete lines and a $\Delta E_\gamma = 0.5 \text{ keV}$ binning. The spectrum is defined so that $I_i(E_\gamma) \Delta E_\gamma$ gives the absolute probability of observing γ rays with energies in the $(E_\gamma - 0.5 \Delta E_\gamma, E_\gamma + 0.5 \Delta E_\gamma)$ interval per decay of the material i .

During the period $t, t + \delta t$, the γ -ray spectrum obtained by adding the contribution of all the radioactive nuclides in the core is given by

$$I(E_\gamma, t, t + \delta t) = \sum_i \lambda_i N_i(t) I_i(E_\gamma) \delta t, \quad (2)$$

TABLE I. Electromagnetic energies (in million electron volts per fission) in decay heat of ^{235}U .

Time interval (s)	Present work	ENDF/B-VII.1 [22]	Dickens [15]	JEFF-3.1 [23]	Average value
1–1800	3.60	4.12	4.10	4.00	4.07
1–9000	4.34	4.84	4.74	4.70	4.76

which can be integrated over time to obtain

$$I(E_\gamma, t_0, t_1) = \sum_i I_i(E_\gamma) \int_{t_0}^{t_1} \lambda_i N_i(t) dt. \quad (3)$$

The mean electromagnetic energy (E_{EEM}) and average γ energy of the spectrum are calculated as

$$E_{\text{EEM}}(t_0, t_1) = \int I(E_\gamma, t_0, t_1) E_\gamma dE_\gamma, \quad (4)$$

$$\langle E_\gamma(t_0, t_1) \rangle = \int I(E_\gamma, t_0, t_1) E_\gamma dE_\gamma / \int I(E_\gamma, t_0, t_1) dE_\gamma. \quad (5)$$

Equations (1) were solved numerically using the fission yields from the JEFF-3.1 library [23] and the decay data from the ENDF/B-VII.1 library [22].

To confirm the correctness of our procedure, we first calculated delayed γ -ray spectra for time intervals $t = 1$ –1800 s and $t = 1$ –9000 s following a single fission event at $t = 0$. These time intervals match the cycling times in our reactor model. Our E_{EEM} values are shown in the second column of Table I. In columns 3 through 5, we compare values obtained by numerical integration of $f(t)$ as given in Refs. [15,22,23]. The last column is an average of these three reference values. Our E_{EEM} values are about 0.40 MeV lower because they are derived from pointwise γ -ray spectra. If we use the E_{EEM} values in the ENDF/B-VII.1 library, which includes the latest TAGS measurements, we obtain $E_{\text{EEM}}(1, 1800) =$

4.03 MeV and $E_{\text{EEM}}(1, 9000) = 4.77$ MeV, in agreement with the average of other results. Because of the pandemonium effect [24], it is a well-known fact that one obtains a lower E_{EEM} value when using pointwise spectra, in this case about 10%.

We are interested in the γ -ray flux in the pulsed cycling mode of the reactor operation, not just for a fission event at $t = 0$. We therefore calculated next the γ -ray spectra during the 0.5-h (1800-s) pulse and during the 2.5-h (9000-s) cooling period, assuming one fission per second during the reactor-on pulse. In these calculations we took $N_i = 0$, that is, a fresh core. The spectra for a 0.15- to 10-MeV energy range are shown in Figs. 2 and 3, the former on a log scale and the latter on a linear scale to show the fine structure of the lower energy portion of the spectrum. The E_{EEM} value for the reactor-on 0- to 1800-s spectrum is 3.49 MeV/fission, with $\langle E_\gamma \rangle$ equal to 0.732 MeV. For the reactor-off 1800- to 10 800-s spectrum, E_{EEM} is equal to 1.24 MeV/fission and $\langle E_\gamma \rangle$ is slightly higher, 0.813 MeV. Adding the spectra gives $E_{\text{EEM}}(0, 10800) = 4.73$ MeV.

Using these E_{EEM} values and knowing the number of fissions per pulse, we can now calculate the prompt, delayed, and equilibrium components of the electromagnetic energy for the reactor-on and reactor-off time intervals. These values are shown in columns 2 through 4 of Table II. The prompt entry corresponds to the energy from prompt fission and neutron-capture γ rays. This is zero when the reactor is off.

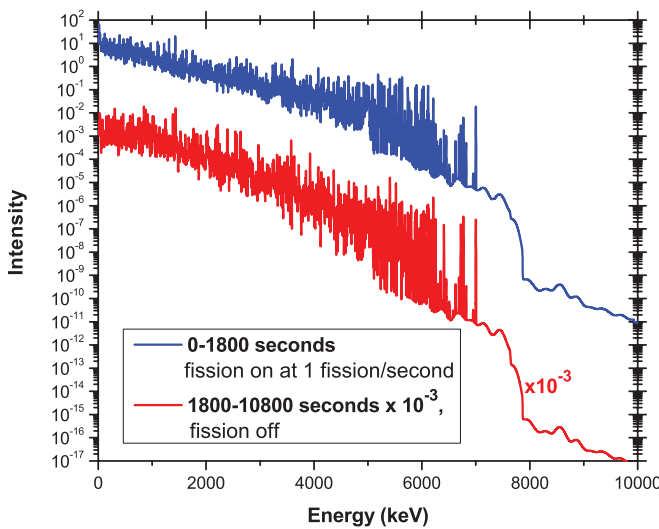


FIG. 2. (Color online) Time-integrated γ -ray spectra in the 0.15- to 10-MeV range for the $T = 0$ –1800 s reactor-on pulse (upper) at one fission/s and for the reactor-off period $T = 1800$ –10 800 (lower), the latter scaled down by a factor of 10^3 for clarity. Counts are per 1-eV energy interval.

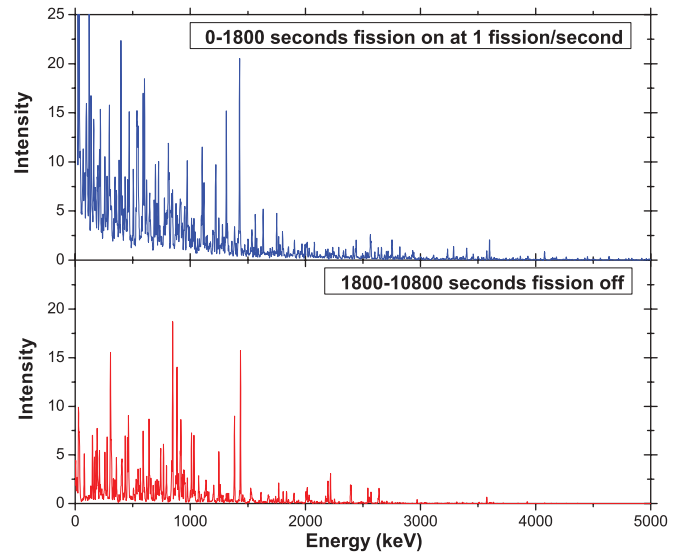


FIG. 3. (Color online) Time-integrated γ -ray spectra in the 0.15- to 5-MeV range for the $T = 0$ –1800 s reactor-on pulse (top) and for the reactor-off period $T = 1800$ –10 800 (bottom). Counts are per 1-eV energy interval. The discrete nature of the spectra is more evident as compared to Fig. 2 but (see text) can still be treated as quasicontinuous for purposes of estimating photoexcitation probabilities.

TABLE II. Electromagnetic energies (in 10^{18} MeV) for the pulsed model of reactor RZ10.

ΔT (s)	Prompt	Delayed	Equilibrium	Energy rate (10^{15} MeV/s)
0–1800	15.14	3.59	1.12	11.03
1800–10 800		1.28	5.62	0.77

The delayed entries are derived from the γ -ray decay E_{EEM} values given earlier. Both prompt and delayed components originate from one single reactor-on pulse of power 18 kW. In addition to these components, there is also equilibrium decay heat associated with fission from the N previous pulses ($N \gg 1$). For our purposes this can be estimated over short periods of time simply by using the standard relation for the power of the after heat compared to the power of the reactor: $P_{\text{heat}} = 0.066 P_{\text{av}}$ [16]. Taking the average thermal power in our model to be $P_{\text{av}} = 3$ kW and noting only half the energy in the after heat is electromagnetic, we then have $P_{\gamma} = 0.033 P_{\text{av}}$, which leads to the values shown in column 4. We see the equilibrium flux within the pulse is a factor of $1.12/3.59 = 0.31$ smaller than the delayed flux within the pulse.

The last column is the energy release per unit time summed over all electromagnetic components. Assuming similar spectral shapes of the components, these latter quantities are proportional to the total γ -ray flux during the reactor-on and reactor-off pulses. We conclude that the flux in time intervals between pulses (1800–10 800 s) will be about 7% of the flux during the 1800-s reactor-on pulse.

IV. CONVERSION OF THE DELAYED γ -RAY SPECTRA TO γ -RAY FLUXES

To estimate the photoexcitation parameters $\lambda_{\gamma,\gamma'}$ in ^{176}Lu it is necessary to know γ -ray fluxes, not simply Ge-detector spectra. The prompt flux is obtained directly as output of MCNP [19]. We get the delayed flux using the γ -ray dose to photon fluence conversion factors published by the International Commission on Radiological Protection (ICRP) [25]. Our conversion assumes that all γ -rays produced in Oklo reactors are absorbed by the active core materials, both fertile and infertile.

The conversion coefficients $k(E)$ are listed in Table III, where the absorbed dose is in units of erg g^{-1} and the photon fluence is in units of $\gamma \text{ cm}^{-2}$. A polynomial fit to these data gives $k(E) = 0.114E^3 - 1.091E^2 + 5.618E - 0.189$ with E in million electron volts.

For the Oklo zone RZ10, the total mass is 60 tons. To convert the reactor-on spectrum of Fig. 2 to a flux, we therefore multiply by the energy E_{γ} , divide by $k(E_{\gamma})$, divide by the total mass of the reactor zone and the 1800-s accumulation time, and normalize to the ^{235}U fission rate $5.71 \times 10^{14} \text{ s}^{-1}$. We multiply this flux by 1.31 to take into account the contribution

of the equilibrium flux. The resulting reactor-on delayed + equilibrium flux, binned in 100-keV intervals, is shown in Fig. 1 and can now be compared to the prompt flux. We see it is typically an order of magnitude smaller. However, at a few energies it does actually exceed the prompt flux.

V. IMPLICATIONS OF γ -RAY FLUX ESTIMATES FOR $^{176}\text{Lu}/^{175}\text{Lu}$ THERMOMETRY

Lutetium thermometry is based on the dependence of the $^{176}\text{Lu}/^{175}\text{Lu}$ isotopic ratio on the operating temperature of a reactor in which ^{176}Lu is burned (and partially restituted) by neutron capture reactions. As detailed in Ref. [9], this process is not described by a single exponential decay constant. However, to set a time scale for judging the impact of the γ -ray flux, we can introduce an effective constant $\lambda_n^{\text{eff}} = 3.7 \times 10^{-13} \text{ s}^{-1}$ (effective half-life of 60 kyr) based on the factor 6.4 reduction in the isotopic ratio over the 160-kyr operating time of RZ10 [5]. Then we write the total constant for disappearance of ^{176}Lu as $\lambda = \lambda_n + \lambda_{\gamma,\gamma'}$, where the second term corresponds to the photoexcitation process as an alternate explanation for ^{176}Lu depletion. We omit the β decay constant for ^{176}Lu $\lambda_{\beta} = 5.8 \times 10^{-19} \text{ s}^{-1}$ because it is by six orders of magnitude less than λ_n^{eff} .

Experimental data [11,12] confirm that long-lived ^{176}Lu in the photon bath of celestial bodies can be partially transformed into metastable ^{176m}Lu by photons with energies around 880, 1060, 1330, and 1660 keV. Higher energy photons may also contribute [26]. These photon energies correspond to excited states of ^{176}Lu with specific spins and parities which allow them to act as mediators for photoexcitation of the isomeric state. The rate $\lambda_{\gamma,\gamma'}(E_i)$ of photoexcitation of the isomeric state ^{176m}Lu in photon inelastic scattering through an intermediate state (IS) at energy E_i is given by

$$\lambda_{\gamma,\gamma'}(E_i) = \int \Phi_{\gamma}(E) \sigma_{\gamma,\gamma'}(E, E_i) dE = \Phi_{\gamma}(E_i) \sigma_{\gamma,\gamma'}^{\text{int}}(E_i). \quad (6)$$

Here $\Phi_{\gamma}(E_i)$ is the differential photon flux at energy E_i having units of $\text{keV}^{-1} \text{ cm}^{-2} \text{ s}^{-1}$, and $\sigma_{\gamma,\gamma'}^{\text{int}}(E_i) = \int \sigma_{\gamma,\gamma'}(E, E_i) dE$ is the integrated cross section for the IS. When several ISs contribute, $\lambda_{\gamma,\gamma'}$ will be a sum over the individual IS contributions.

In writing the rate on the right as the product of two factors we are implicitly assuming the flux is continuous and varying slowly over the narrow resonance energy E_i . This is true in stellar environments and, for example, in bremsstrahlung experiments. It is not necessarily the case in our situation, where the photon spectra are made up from a sum over many discrete γ -ray lines. However, our fluxes propagate in the dense environment of the Oklo reactors and as discussed by von Neumann-Cosel *et al.* [27], Compton scattering can broaden otherwise discrete spectra quite significantly. The

TABLE III. Fluence-to-dose conversion coefficients $k(E_{\gamma})$ for γ rays with energy E_{γ} [25].

E_{γ} (keV)	100	200	300	400	500	600	800	1000	1500	2000	3000	4000
$k(E_{\gamma})$ ($10^{-8} \text{ erg g}^{-1}/\gamma \text{ cm}^{-2}$)	0.37	0.86	1.38	1.89	2.38	2.84	3.69	4.47	6.14	7.55	9.96	12.10

MCNP code models Compton scattering, pair production, and electron bremsstrahlung fully, leading to the continuous prompt spectrum shown in Fig. 1. The delayed spectra show more structure, but for purposes of estimating upper bounds on the photoexcitation process we assume our 100-keV averaging procedure will serve as a useful approximation.

Reported values of the photoexcitation cross sections given in the literature include $\sigma_{\gamma,\gamma'}^{\text{int}}(E_\gamma) = 33.4 \text{ mb eV}$ for $E_\gamma = 839 \text{ keV}$ (this is an upper limit in Ref. [12], for a laboratory environment, as opposed to a fully ionized environment), and higher values $\sigma_{\gamma,\gamma'}^{\text{int}}(E_\gamma) = 140 \text{ mb keV}$ and 350 mb keV , for 4- and 6-MeV bremsstrahlung irradiations respectively, with an assumed IS energy of 2.125 MeV [26].

With these cross sections and the fluxes $\Phi_\gamma(E)$ of Fig. 1 at hand, we can now calculate $\lambda_{\gamma,\gamma'}$ for Oklo reactor RZ10. Taking into account the pulse structure, we use a weighted average flux consisting of 1/6 of the sum of the prompt, delayed, and equilibrium fluxes while the reactor is on and 5/6 of 7% of this sum while the reactor is off.

The option of $E_\gamma = 839 \text{ keV}$, with a total spectral flux of $0.86 \times 10^6 \gamma \text{ cm}^{-2} \text{ s}^{-1} \text{ keV}^{-1}$, leads to $\lambda_{\gamma,\gamma'} = 0.26 \times 10^{-22} \text{ s}^{-1}$, which is negligible. The 6-MeV bremsstrahlung option with $E_\gamma = 2.1 \text{ MeV}$ has a total spectral flux of $1.9 \times 10^5 \gamma \text{ cm}^{-2} \text{ s}^{-1} \text{ keV}^{-1}$ and gives $\lambda_{\gamma,\gamma'} = 6.8 \times 10^{-20} \text{ s}^{-1}$. However, even this value is less than the λ_n^{eff} by seven orders of magnitude. We conclude that destruction of ^{176}Lu in the Oklo reactors is not influenced by any part of the reactor-on photon flux.

After complete shutdown, the power of the γ -ray decay heat decreases approximately as $t^{-0.3}$ [16], reaching about 1% of the equilibrium value after a year. At this point it can be ignored. We conclude therefore that the decay heat is also not able to change the lutetium isotopic ratio even over the long period when the reactor has been shut down.

The particular values we have found are specific to the uniform pulsed mode of operation that we have assumed. However, the burn rate for steady-state reactor operation will not be much different since our result is determined mainly by the prompt flux, which scales inversely with the live time of the reactor. Absent a photoexcitation cross section larger by many orders of magnitude through as yet undetermined levels, we see the photon intensities in the reactor are insufficient to alter the $^{176}\text{Lu}/^{175}\text{Lu}$ isotopic ratios associated with neutron transmutation.

VI. CONCLUSIONS

We have developed realistic models of the prompt and delayed γ -ray fluxes in Oklo natural nuclear reactors, taking advantage of recent releases of the databases and methodology that accurately represent short-time decay heat in fission processes. We have compared ^{176}Lu transmutation rates associated with photoexcitation to transmutation rates associated with neutron capture processes. In contrast to astrophysical processes, we find $^{176}\text{Lu}/^{175}\text{Lu}$ isotopic ratios in Oklo are not influenced by decay heat electromagnetic radiation, either during reactor operation or after reactor shutdown. Lutetium thermometry, as recently studied [9], is therefore applicable to analyses of Oklo reactor data.

ACKNOWLEDGMENTS

This work was supported by the US Department of Energy, Office of Nuclear Physics, under Grant No. DE-FG02-97ER41041 (North Carolina State University) and under Contract No. DE-AC02-98CH10886 with Brookhaven Science Associates (NNDC).

-
- [1] R. Naudet, *Oklo: des Réacteurs Nucléaires Fossiles* (Eyrolles, Paris, 1991).
 - [2] A. Shlyakhter, *Nature (London)* **264**, 340 (1976).
 - [3] Y. Fujii, A. Iwamoto, T. Fukahori, T. Ohnuki, M. Nakagawa, H. Hidaka, Y. Oura, and P. Moeller, *Nucl. Phys. B* **573**, 377 (2001), revisited in [arXiv:hep-ph/0205206](https://arxiv.org/abs/hep-ph/0205206).
 - [4] T. Damour and F. Dyson, *Nucl. Phys. B* **480**, 37 (1996).
 - [5] C. R. Gould, E. I. Sharapov, and S. K. Lamoreaux, *Phys. Rev. C* **74**, 024607 (2006).
 - [6] Yu. V. Petrov, A. I. Nazarov, M. S. Onegin, V. Yu. Petrov, and E. G. Sakhnovsky, *Phys. Rev. C* **74**, 064610 (2006).
 - [7] M. S. Onegin, [arXiv:1010.6299v1](https://arxiv.org/abs/1010.6299v1) [nucl-th].
 - [8] J. K. Webb, J. A. King, M. T. Murphy, V. V. Flambaum, R. F. Carswell, and M. B. Bainbridge, *Phys. Rev. Lett.* **107**, 191101 (2011).
 - [9] C. R. Gould and E. I. Sharapov, *Phys. Rev. C* **85**, 024610 (2012).
 - [10] Abundance and lifetime data from the National Nuclear Data Center [www.nndc.bnl.gov].
 - [11] K. Thrane, J. N. Connelly, M. Bizzarro, B. S. Meyer, and L. S. The, *Astrophys. J.* **717**, 861 (2010).
 - [12] P. Mohr, S. Bisterzo, R. Gallino, F. Käppeler, U. Kneissl, and N. Winckler, *Phys. Rev. C* **79**, 045804 (2009).
 - [13] K. Way and E. P. Wigner, *Phys. Rev.* **73**, 1318 (1948).
 - [14] A. Tobias, *Prog. Nucl. Energy* **5**, 1 (1980).
 - [15] J. K. Dickens, Conf-860906-9, Oak Ridge National Laboratory, Oak Ridge, TN, 1986 (unpublished).
 - [16] S. Glasstone and A. Sesonske, *Nuclear Reactor Engineering*, 3rd ed. (Van Nostrand Reinhold, New York, 1981).
 - [17] A. Algora, D. Jordan, J. L. Tain, B. Rubio, J. Agramunt, A. B. Perez-Cerdan, F. Molina, L. Caballero, E. Nacher, A. Krasznahorkay, M. D. Hunyadi, J. Gulyas, A. Vitez, M. Csatos, L. Csige, J. Aysto, H. Penttila, I. D. Moore, T. Eronen, A. Jokinen, A. Nieminen, J. Hakala, P. Karvonen, A. Kankainen, A. Saastamoinen, J. Rissanen, T. Kessler, C. Weber, J. Ronkainen, S. Rahaman, V. Elomaa, S. Rinta-Antila, U. Hager, T. Sonoda, K. Burkard, W. Huller, L. Batist, W. Gelletly, A. L. Nichols, T. Yoshida, A. A. Sonzogno, and K. Perajarvi, *Phys. Rev. Lett.* **105**, 202501 (2010).
 - [18] T. D. Johnson, A. Sonzogno, and E. McClutchan, *Bull. Am. Phys. Soc.* **56**, 12 (2011).

- [19] J. F. Briesmeister, ed. MCNPTM—A *general Monte Carlo N-particle transport code, version 4C*, LA-13709-M (Los Alamos National Laboratory, Los Alamos, 2000).
- [20] H. Hidaka and P. Holliger, *Geochim. Cosmochim. Acta* **62**, 891 (1998).
- [21] A. P. Meshik, C. M. Hohenberg, and O. V. Pravdivtseva, *Phys. Rev. Lett.* **93**, 182302 (2004).
- [22] M. B. Chadwick, M. Herman, P. Oblozinsky *et al.*, *Nucl. Data Sheets* **112**, 2887 (2011).
- [23] M. A. Kellet, O. Bersillon, and R. W. Mills, OECD NEA 6287 Report, 2009 (unpublished).
- [24] J. C. Hardy, L. C. Carraz, B. Jonson, and P. G. Hansen, *Phys. Lett. B* **71**, 307 (1977).
- [25] Annals of the ICRP, Vol. 26-3, 159 (1996).
- [26] J. J. Carroll, M. J. Byrd, D. G. Richmond, T. W. Sinor, K. N. Taylor, W. L. Hodge, Y. Paiss, C. D. Eberhard, J. A. Anderson, C. B. Collins, E. C. Scarbrough, P. P. Antich, F. J. Agee, D. Davis, G. A. Huttlin, K. G. Kerris, M. S. Litz, and D. A. Whittaker, *Phys. Rev. C* **43**, 1238 (1991).
- [27] P. von Neumann-Cosel, A. Richter, J. J. Carroll, and C. B. Collins, *Phys. Rev. C* **44**, 554 (1991).